THE JOURNAL OF PHYSICAL CHEMISTRY B

Article

pubs.acs.org/JPCB

Unexpected Absorbance Enhancement upon Clustering Dyes in a Polymer Matrix

Adriana Gelover-Santiago,[†] Michael A. Fowler,[§] Jamie Yip,[§] Jean Duhamel,*[,§] Guillermina Burillo,*[,‡] and Ernesto Rivera*[,†]

[†]Instituto de Investigaciones en Materiales and [‡]Instituto de Ciencias Nucleares, Universidad Nacional Autónoma de México, Circuito Exterior S/N, Ciudad Universitaria, Coyoacán, 04510, México

[§]Institute for Polymer Research, Department of Chemistry, University of Waterloo, Waterloo, Ontario N2L 3G1, Canada

Supporting Information

ABSTRACT: PE films grafted with poly(methyl acrylate) and labeled with pyrene groups were obtained by irradiation with γ-rays in the presence of acryloyl chloride and further reacting them with 1-pyrenebutanol or 1-pyrenemethylamine. Characterization of the polymer films benefited from the dual use of the pyrene probe as an indicator of, first, polymer chain dynamics by monitoring pyrene excimer formation by fluorescence and, second, polymer morphology by staining the pyrene-rich domains of the films with RuO_4 for scanning electron microscopy (SEM). The grafted polymers labeled with 1-pyrenemethylamine showed much stronger absorbance than those labeled with 1-pyrenebutanol despite having similar pyrene contents. The fluorescence spectra of the grafted polymers labeled with 1-pyrenebutanol exhibited monomer emission, whereas those labeled with 1-pyrenemethylamine exhibited exclusively excimer emission. These dramatic differences could be accounted for by noting that labeling of the grafted poly(acryloyl chloride) with 1-pyrenemethylamine results in cross-linking of the polymer matrix, with an associated enhancement of the concentration of pyrene in the cross-linked domains, which was confirmed by SEM. Formation of discrete domains in the polymer film can induce multiple scattering at the domain boundaries which lengthens the path of light in the film and increases absorption of the light by the tightly packed pyrene-rich domains. Implementation of this effect for fabrication of plastic color filters should generate more efficient filters which should find numerous practical applications.

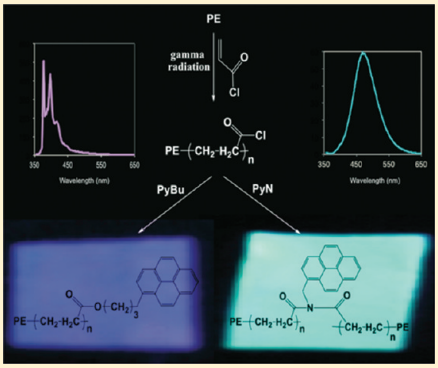

INTRODUCTION

Plastic color filters or polymers capable of blocking light at specific wavelengths are of particular interest to numerous commercial applications from high-tech light-emitting devices for flat displays to more mundane ones such as sunglasses or tinted plastic containers designed to hold light-sensitive material.[1−3] These properties can be achieved by either blending a dye into the plastic[1] or covalently incorporating the dye into the polymer.[3,4] The latter option is better suited for applications where the plastic comes into contact with a liquid as covalent attachment of the dye to the polymer reduces the risk of the dye being released from the plastic into the liquid.[5] As with any commercial application, procedures that minimize the amount of chemicals that need to be applied to induce a modification, in this case the amount of dye that needs to be attached to the polymer, are highly valuable since they reduce cost, eventual contamination of the chemical stored in the plastic container, and the thickness of the plastic color filter. With this background in mind, this report presents observations indicating that for a same loading of a dye into a polymer matrix attachment of a dye in a clustered manner onto a polymer matrix leads to a dramatic enhancement in the absorbance of the sample compared to a sample where the dye is attached uniformly throughout the polymer matrix. These conclusions were reached by characterizing pyrene-labeled polyethylene (PE) films with a wide array of techniques.

Since PE is a plastic commonly used in packaging applications, PE films were chemically modified to introduce reactive groups which could be employed at a later stage for covalent attachment of an aromatic dye. The modified PE films were prepared by initiating polymerization of acryloyl chloride (AC) in the presence of the PE plates with γ-radiation[6−9] and reacting the poly(acryloyl chloride) with, first, either 1-pyrenylbutanol (AC-*g*-PE-PyBu) or 1-pyrenemethylamine (AC-*g*-PE-PyN) and, second, methanol. The chromophore pyrene was selected as its self-aggregation results in formation of an excimer whose easy detection by fluorescence provides evidence of the level of clustering of the pyrene pendants.[10,11] Polymer samples were characterized by FTIR spectroscopy and thermal analysis (thermogravimetry and differential scanning calorimetry) and swelling, and the photophysical properties (UV−vis absorption and steady-state and time-resolved

Received: September 7, 2011
Revised: April 10, 2012
Published: May 17, 2012

fluorescence) of the modified films were investigated. The morphology of the films interior was characterized by scanning electron microscopy (SEM).

Although the modified PE films had a similar pyrene content as determined by weight, their absorbance and fluorescence spectra were completely different. The films labeled with PyBu showed a relatively low absorbance and only pyrene monomer fluorescence; the films labeled with PyN showed much larger absorbance and pyrene excimer fluorescence only. The partitioning of the pyrene pendants into pyrene-rich domains induced via formation of imide bridges for the AC-*g*-PE-PyN films was inferred from fluorescence measurements and confirmed by SEM. While pyrene clustering for the films prepared with PyN rationalized excimer formation in these samples, the large enhancement in absorbance was, on the other hand, somewhat unexpected as formation of pyrene aggregates is known to reduce the molar absorbance coefficient of a pyrenyl unit,[12,13] and thus, the overall absorbance of the sample should decrease contrary to what was observed experimentally. Nevertheless, the strong enhancement in absorbance appears to be a direct consequence of the clustering of the dyes into pyrene-rich domains inside the polymer matrix, an effect that is expected to find important practical applications.

EXPERIMENTAL SECTION

Materials. Low-density PE plates with dimensions of 1 cm × 5 cm × 0.07 mm, a density of 0.92 g/cm^3, and a crystallinity of 50% were purchased from Goodfellow, England. Acryloyl chloride (AC), toluene, methylene chloride, and methanol used in the preparation of the grafted polymers were purchased from Aldrich. AC was purified by distillation at reduced pressure, whereas toluene, methylene chloride, and methanol were distilled at atmospheric pressure once dried with $CaCl_2$. After purification, polymer films, reagents, and solvents were stored in a desiccator over $CaCl_2$ in order to avoid any contact with moisture.

Preparation of the Grafted Polymers. PE plates were washed with methanol and further dried under vacuum until a constant weight was attained; then they were placed in glass ampules containing AC solutions in toluene. The ampules were purged under vacuum by repeated freezing and thawing cycles. Then, they were sealed and irradiated with a ^{60}Co γ-source (Gamma beam 651 PT, Nordion International Inc.) at different doses from 2 to 16 kGy and dose rates of 9.5 and 8.7 kGy/h for the AC-*g*-PE-PyBu and AC-*g*-PE-PyN samples, respectively. Decay factors for the ^{60}Co half-life of 5.272 years were obtained from tables provided by 'Puridec, Irradiation Technologies'. After irradiation, the grafted samples were washed with CH_2Cl_2 for 24 h in order to eliminate residual monomer and poly(acryloyl chloride) byproduct present as occlusions in the films. Immediately after, the PE plates grafted with poly(acryloyl chloride) were placed in CH_2Cl_2 solutions of the corresponding pyrene derivative in the presence of triethylamine. The mixtures were stirred for 24 h. Afterwards, the samples were washed with MeOH in the presence of triethylamine to remove the unreacted pyrene derivative and to convert the remaining acid chloride groups into methyl esters. Samples were dried under vacuum until a constant weight was reached. Films esterified with methanol only were used as reference to calculate the amount of grafted AC. Therefore, the percentage of grafted AC was determined from the weight increase of the esterified films by comparing it to that of the starting PE plate. The yield of grafting (Grafting%) was determined using eq 1

$$\text{Grafting\%} = 100 \times \frac{W - W_o}{W_o} \quad (1)$$

where W is the weight of the grafted polymer esterified with methanol and W_o is the weight of the original PE plate. The amount of pyrene attached onto the film characterized by the percentage Py-Grafting% was also calculated by weight difference using eq 2

$$\text{Py-Grafting\%} = 100 \times \frac{W_p - W}{W} \quad (2)$$

where W_p is the weight of the final grafted polymer labeled with pyrene and W is the weight of the grafted polymer totally esterified with methanol which was used to determine Grafting% in eq 1.

Characterization. FTIR spectra were recorded on a Nicolet model 510P spectrometer. The thermal properties of the films were measured on a TA Instrument, model SDTQ 600. Thermal stability of the compounds was studied by thermogravimetric analysis (TGA) from 0 to 600 °C. Melting points (T_m) were determined by differential scanning calorimetry (DSC). A heating rate of 10 °C/min was used for both the TGA and the DSC analyses.

Absorption spectra of the grafted polymers were recorded on a CARY 100 Bio UV−Vis spectrophotometer by placing the films between two quartz plates. Steady-state fluorescence measurements were performed on a Photon Technology International (PTI) LS-100 steady-state fluorometer with an Ushio UXL-75Xe Xenon arc flash lamp and PTI 814 photomultiplier detection system. All fluorescence spectra were acquired with the front-face geometry.[14] Emission of the films in the dry state was recorded without degassing the sample. For experiments with the films swollen in acetone, the films were mounted onto a triangular fluorescence cell for front-face fluorescence measurements, which was filled with acetone and placed in an Optistat DN cryostat from Oxford Instruments. The cryostat was then mounted onto the steady-state (and later onto the time-resolved) fluorometer to acquire fluorescence spectra of the films in acetone. The cryostat was operated at room temperature and under nitrogen atmosphere to prevent oxygen quenching of the films swollen in acetone. Fluorescence decays were acquired with an IBH Ltd. time-resolved fluorometer equipped with an IBH 340 nm NanoLED. The films were excited at 344 nm, and the monomer and excimer fluorescence decays were acquired at 375 and 510 nm, respectively. Light scattering was blocked off from reaching the detector with cut off filters at 370 and 495 nm, respectively. All fluorescence decays had 20 000 counts at their maximum. The instrument response function was determined with a Ludox solution. Decays were fitted with a sum of exponentials. Optimization of the pre-exponential factors and decay times was accomplished with the Marquardt−Levenberg algorithm.[15] The quality of the fit was determined from the χ^2 parameter ($\chi^2 < 1.30$) and the random distribution of the residuals and the autocorrelation of the residuals. Gel permeation chromatography measurements were performed using a Jordi X-stream H_2O MS(LS) mixed bed column, a Waters 510 HPLC pump, an Agilent G1321A fluorescence detector, a Minidawn light-scattering detector (490 nm), and a Waters 410 differential refractometer.

dx.doi.org/10.1021/jp208646b | J. Phys. Chem. B 2012, 116, 6203−6214

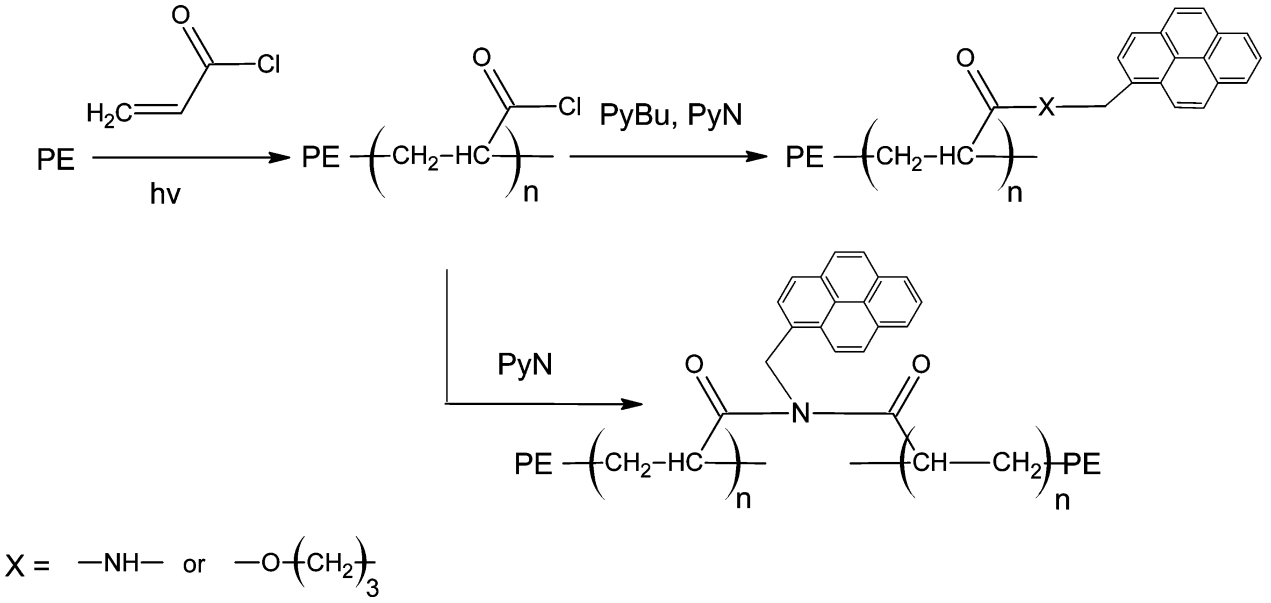

Figure 1. Reaction scheme for the grafting and pyrene labeling of the PE films.

The cross-section of the films were imaged by scanning electron microscopy (SEM) with a LEO 1530 field emission SEM equipped with a backscatter detector using a voltage of EHT = 5.0 kV. Samples were freeze fractured under liquid nitrogen and stained with RuO_4.

RESULTS AND DISCUSSION

Preparation of Grafted Polymers. Preparation of the grafted polymers labeled with 1-pyrenebutanol (AC-*g*-PE-PyBu) and 1-pyrenemethylamine (AC-*g*-PE-PyN) was carried out according to the method illustrated in Figure 1.

First, PE polymer plates were exposed to γ-radiation in the presence of an AC solution in toluene (50:50 vol %) in sealed ampules to yield the corresponding precursor polymers AC-*g*-PE. Different radiation doses from 2 to 16 kGy were applied in order to obtain polymers with different grafting percentages. Further reaction of the precursor polymers with the appropriate pyrene derivative in the presence of triethylamine leads to formation of the desired functionalized polymers. The yield of grafting (Grafting%) was determined using eq 1. The amount of pyrene attached onto the film characterized by the percentage Py-Grafting% was also calculated by weight difference using eq 2. Figure 2 shows a plot of the amount of acryloyl chloride grafted onto PE as a function of the radiation dose. As expected, the amount of acryloyl chloride grafted onto the PE plates increases proportionally with increasing applied dose within experimental error.

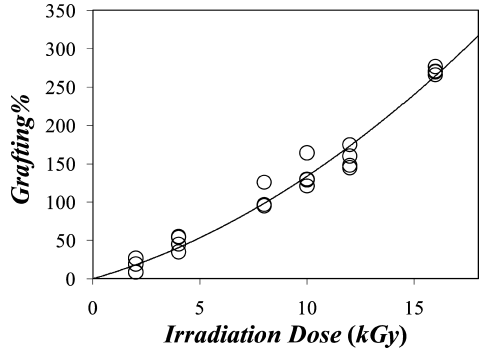

Figure 2. Plot of Grafting% in eq 1 as a function of irradiation dose.

The weight percentage Py-Grafting% of pyrene derivative covalently attached onto the films was determined and is listed in Table 1. Py-Grafting% remained more or less constant with

Table 1. Weight Percentage (Py-Grafting% calculated with eq 2) and Molar Fraction (x calculated with eq 3) of Pyrene Label Per Methyl Acrylate Structural Unit

sample	Py-Grafting%	x (without cross-links)	$x/2^b$ (with cross-links)
AC-*g*-PE-PyBu-2kGy[a]	46[a]	1.00[a]	NA
AC-*g*-PE-PyBu-4kGy	18	0.19	NA
AC-*g*-PE-PyBu-8kGy	23	0.15	NA
AC-*g*-PE-PyBu-10kGy	30	0.17	NA
AC-*g*-PE-PyBu-12kGy	13	0.08	NA
AC-*g*-PE-PyBu-16kGy	20	0.10	NA
AC-*g*-PE-PyN-2kGy[a]	24[a]	0.49[a]	0.43[a]
AC-*g*-PE-PyN-4kGy	31	0.38	0.33
AC-*g*-PE-PyN-8kGy	36	0.32	0.28
AC-*g*-PE-PyN-10kGy	33	0.25	0.22
AC-*g*-PE-PyN-12kGy	17	0.12	0.11
AC-*g*-PE-PyN-16kGy	38	0.23	0.20

[a]The small level of grafting in this sample makes the measure of the weight (W_P) in eq 2 unreliable and the parameters derived from W_P. [b]All 1-pyrenemethylamine derivatives are assumed to react with two acryloyl chloride structural units. x represents the molar fraction of acryloyl chloride which have reacted. $x/2$ represents the molar fraction of pyrene label per acryloyl chloride unit.

dx.doi.org/10.1021/jp208646b | J. Phys. Chem. B 2012, 116, 6203–6214

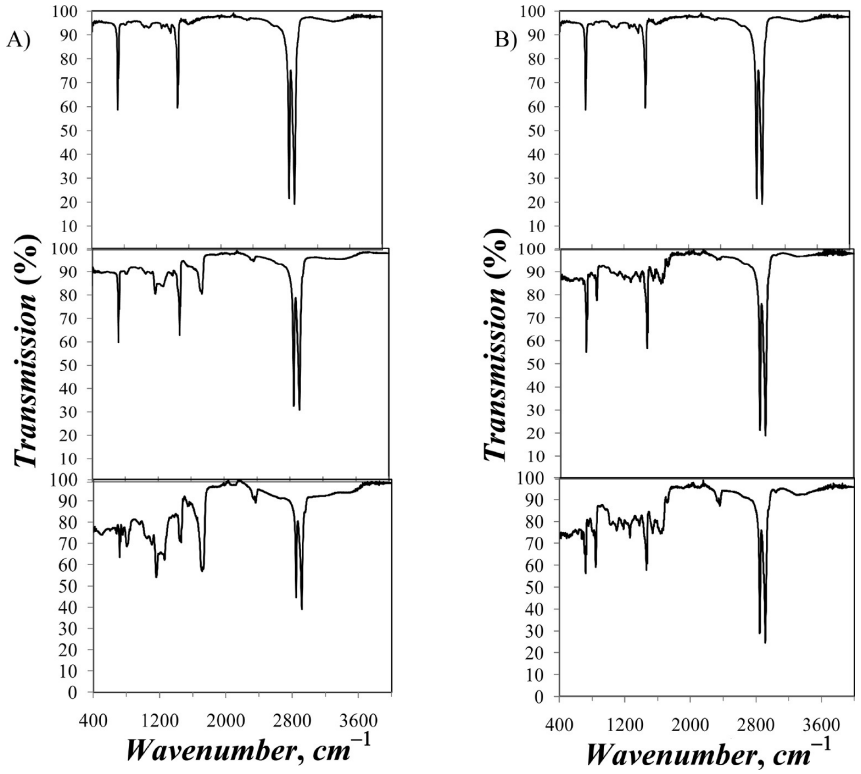

Figure 3. FTIR spectra of from top to bottom: (A) PE, AC-*g*-PE-PyBu-2kGy and AC-*g*-PE-PyBu-10kGy and (B) PE, AC-*g*-PE-PyN-2kGy and AC-*g*-PE-PyN-10kGy.

irradiation dose at 21 ± 12 and 31 ± 8 for the AC-*g*-PE-PyBu and AC-*g*-PE-PyN samples, respectively, corresponding to molar fractions of pyrene-labeled poly(methyl acrylate) equal to 0.14 ± 0.05 and 0.26 ± 0.10 assuming that no cross-linking was taking place.

In turn, the percentages Grafting% and Py-Grafting% can be used to determine the molar fraction x of acrylate monomers that reacted with a pyrene derivative according to eq 3

$$x = \frac{M_{MA}}{M_{MA-Py} - z \times M_{MA}} \times \frac{\text{Py-Grafting\%} \times (\text{Grafting\%} - 100)}{100 \times \text{Grafting\%}} \quad (3)$$

The parameter z in eq 3 equals 1 or 2 depending on whether none or all 1-pyrenemethylamine used to label the films results in a cross-link. The ratio x/z represents the molar fraction of pyrene derivative per methyl acrylate structural unit. The molar masses M_{MA} and M_{MPy} are those of the methyl acrylate (M_{MA} = 86 g·mol^{-1}) and pyrene-labeled monomers, respectively. M_{MPy} equals 324, 285, and 339 g·mol^{-1} depending on whether the films were labeled with 1-pyrenebutanol, 1-pyrenemethylamine with no cross-linking, and 1-pyrenemethylamine with complete cross-linking, respectively.

The molar fraction of 1-pyrenemethylamine per acryloyl chloride unit ($x/2$) was also calculated with eq 3 using z = 2 assuming that all 1-pyrenemethylamines would result in formation of an imide bridge. The results listed in Table 1 indicate that the molar fraction of pyrene per acrylate unit does not change much whether cross-linking occurs or not. It can also be concluded from the data listed in Table 1 that at least 8 mol % of the acrylate units in the modified films bear a pyrene label. Even this lowest level of pyrene labeling would result in substantial pyrene excimer formation for pyrene-labeled poly(methyl acrylate) in an organic solvent like tetrahydrofuran.[16]

FTIR spectra of the nongrafted polymers used as starting materials and those of the modified polymer films were acquired in order to confirm incorporation of the different pyrene derivatives into the polymer plates (Figure 3). Figure 3A shows FTIR spectra of PE, AC-*g*-PE-PyBu-2kGy, and AC-*g*-PE-PyBu-10kGy. Spectra of the grafted polymers exhibited two bands at 2846 and 2913 cm^{-1}, which correspond to the methylene groups. An additional band due to the carbonyl of the ester group of the grafted AC was observed at 1720 cm^{-1}. Other stretching bands at 1261 and 1162 cm^{-1} corresponding to the C−O bond of the ester groups were also seen. Finally, a band at 808 cm^{-1} due to the =C−H out-of-plane bond of the aromatic rings is also observed.

Another series of polymer films containing 1-pyrenemethylamine (AC-*g*-PE-PyN) was synthesized and characterized using the same method. Figure 3B shows FTIR spectra of PE, AC-*g*-PE-PyN-2kGy, and AC-*g*-PE-PyN-10kGy. FTIR spectra of the polymers AC-*g*-PE-PyN exhibited two bands at 3330 and 2915 cm^{-1} due to the N−H and CH_2 groups, respectively, followed by two bands at 1717 and 1651 cm^{-1} due to the carbonyl of the imide and amide, respectively. Moreover, another band was observed at 1534 cm^{-1} due to the N−H group followed by a band at 1281 cm^{-1} due to the C−N bond of the amine. Finally, a series of bands was observed at 1159, 1110, and 1041 cm^{-1} followed by two bands at 848 and 719 cm^{-1} due to =C−H out of plane. The ratio of the absorption bands gives a qualitative measure of the grafting degree in each polymer.

Thermal Properties of the Grafted Polymers. The thermal properties of the grafted polymer films were studied by TGA and DSC with a heating rate of 10 °C/min. TGA curves

dx.doi.org/10.1021/jp208646b | J. Phys. Chem. B 2012, 116, 6203−6214

of the AC-*g*-PE-PyBu samples are shown in Figure 4. The nongrafted PE exhibited good thermal stability with a T_{10} value

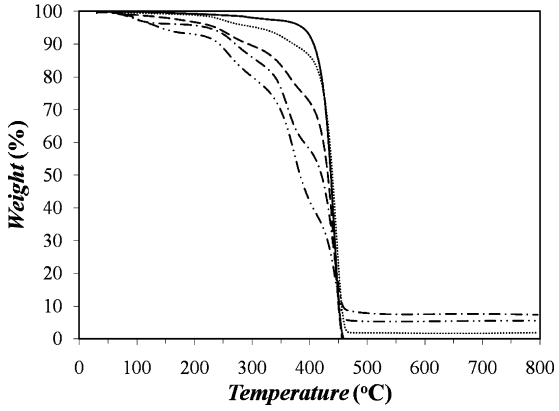

Figure 4. TGA curves of PE (—) and the AC-*g*-PE-PyBu films irradiated with 2 (···), 4 (---), 10 (–·–), and 16 (–···–) kGy.

of 407 °C. Drastic degradation of the polymer was observed between 370 and 490 °C. In contrast, the AC-*g*-PE-PyBu samples showed a worse thermal stability than the nongrafted PE films with T_{10} values varying between 243 and 372 °C. The thermal stability of the films was found to decrease with increasing amount of pyrene labeling. The pyrene label is responsible for the decrease in thermal stability as pyrene itself shows a T_{10} value of 190 °C.[17]

On the other hand, the AC-*g*-PE-PyN polymers exhibited slightly lower thermal stability with respect to the AC-*g*-PE-PyBu films with T_{10} values ranging from 365 to 156 °C. The similar thermal stability of the AC-*g*-PE-PyN films is congruent as this series of films has the same chemical composition as the AC-*g*-PE-PyBu films, namely, pyrene-labeled poly(methyl acrylate) grafted onto a PE plate. Moreover, the melting points of the AC-*g*-PE-PyBu and AC-*g*-PE-PyN samples were determined by DSC (not shown). The polymers exhibited a melting point similar to that of the nongrafted PE (T_m = 111 °C). Therefore, it can be concluded that the grafting process did not alter significantly the nature of the crystalline microdomains of the PE matrix. A similar behavior was observed for synthesis of analogous polymers bearing azobenzene units.[18]

Photophysical Properties of the Grafted Polymers in the Dry Films. Absorption spectra of all films were acquired and are shown in Figure 5. AC-*g*-PE-PyBu films with low pyrene content, samples AC-*g*-PE-PyBu-2kGy and AC-*g*-PE-PyBu-4kGy, showed well-structured absorption bands at 315, 329, and 345 nm (Figure 5A) characteristic of the $S_2 \leftarrow S_0$ transition of the pyrene groups.[19] Films prepared with larger irradiation doses were grafted with larger amounts of poly(acryloyl chloride) (see Figure 2) and, consequently, contained larger amounts of pyrene label. This resulted in a pyrene absorbance that was too strong to be measured with the spectrophotometer.

When the absorption measurements were repeated with the AC-*g*-PE-PyN samples, much larger absorbances were obtained (Figure 5B). In fact, the sharp $S_2 \leftarrow S_0$ absorption bands in the 310–345 nm range were so strong that they could not be resolved with our instrument. Only the typically weak 0–0 transition at 375 nm could be resolved in the absorption spectra showing an increased absorbance with increasing radiation dose. The strikingly different results obtained by UV–vis absorption for the AC-*g*-PE-PyBu and AC-*g*-PE-PyN samples cannot be due to differences in pyrene contents. According to the yield of acryloyl chloride grafting (Py-Grafting%) and the molar fraction of pyrene derivative attached per acryloyl chloride unit, differences in the pyrene content of the films listed in Table 1 cannot account for the dramatic increase in absorbance observed for the AC-*g*-PE-PyN films. We suspect that these differences in absorbance are due to differences in the distribution of the pyrene labels in the polymer matrix. Experiments conducted hereafter support this assumption.

The fluorescence spectra of the AC-*g*-PE-PyBu and AC-*g*-PE-PyN films were acquired and are shown in Figure 6. As for the absorbance results shown in Figure 5, the AC-*g*-PE-PyBu and AC-*g*-PE-PyN samples yield opposite trends. Whereas all AC-*g*-PE-PyBu films exhibited the typical emission of the pyrene monomer in Figure 6A, all AC-*g*-PE-PyN films exhibited no monomer emission in Figure 6B but rather the broad structureless emission typical of the pyrene excimer. These results were unexpected as the pyrene contents of both films (Table 1) are not different enough to yield such opposite trends. If the solid matrix of the dry films was to prevent excimer formation for the AC-*g*-PE-PyBu samples with an average *x* value of 0.14, increasing this average value to 0.26 for the AC-*g*-PE-PyN films would not be expected to result in the excimer-only emission observed in the fluorescence spectra shown in Figure 6B.

Fluorescence decays of the pyrene monomer and excimer were acquired for all films in the dry state. They were fitted with a sum of exponentials whose pre-exponential factors and decay times are listed in Table 2. These fits were conducted in an effort to describe the main features of the fluorescence

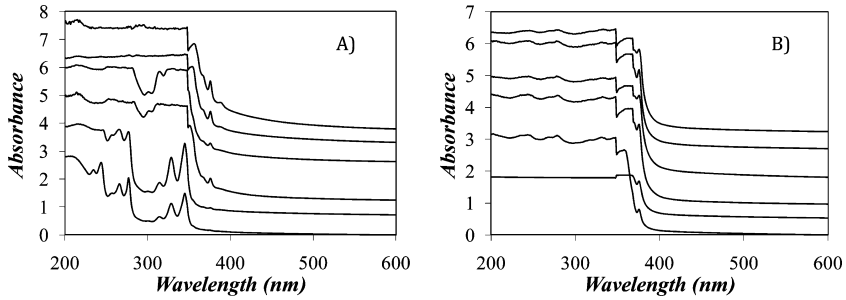

Figure 5. UV–vis absorption spectra for (A) AC-*g*-PE-PyBu films translated by 0, 0.5, 1.0, 2.5, 3.0, and 3.5 absorbance units for films irradiated with 2, 4, 8, 10, 12, and 16 kGy, respectively, and (B) AC-*g*-PE-PyN films translated by 0, 0.3, 0.8, 1.5, 2.5, and 3 absorbance units for films irradiated with 2, 4, 8, 10, 12, and 16 kGy, respectively.

dx.doi.org/10.1021/jp208646b | J. Phys. Chem. B 2012, 116, 6203–6214

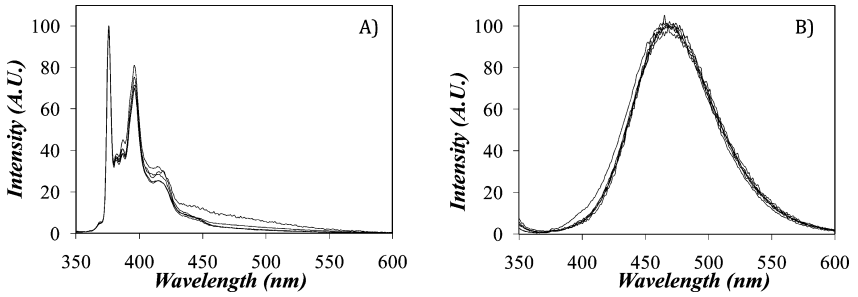

Figure 6. Fluorescence spectra of the AC-*g*-PE-PyBu (A) and AC-*g*-PE-PyN (B) films in the dry state normalized at 376 and 470 nm, respectively. λ_{ex} = 344 nm.

Table 2. Pre-Exponential and Decay Times Retrieved from Analysis of the Time-Resolved Fluorescence Decays of AC-*g*-PE-PyBu and AC-*g*-PE-PyN in the Dry State with a Sum of Exponentials for the Monomer (λ_{ex} = 344, λ_{em} = 375 nm) and Excimer (λ_{ex} = 344, λ_{em} = 510 nm)

	dose (kGy)		τ_1 (ns)	A_1	τ_2 (ns)	A_2	τ_3 (ns)	A_3	τ_4 (ns)	A_4	A_{E-}/A_{E+}	χ^2
AC-*g*-PE-PyBu	2	M	18.1	0.25	81.9	0.27	176	0.48				1.10
		E	5.0	0.46	16.0	0.32	64	0.13	168	0.09	0	1.15
	4	M	13.8	0.21	73.3	0.30	170	0.49				1.00
		E	5.5	0.46	16.8	0.30	64	0.14	164	0.11	0	1.16
	8	M	11.2	0.30	55.6	0.40	138	0.30				1.12
		E	7.7	0.24	26.8	0.23	62	0.42	135	0.11	0	0.89
	10	M	13.3	0.18	65.5	0.36	153	0.46				0.97
		E	10.5	0.45	38.5	0.26	95	0.18	165	0.11	0	0.92
	12	M	14.6	0.19	59.8	0.38	131	0.42				0.93
		E	3.6	−0.19	30.1	0.12	67	0.53	134	0.35	−0.19	1.00
	16	M	12.6	0.21	53.9	0.42	121	0.37				1.16
		E	4.8	−0.11	19.2	0.27	61	0.48	125	0.25	−0.11	1.03
AC-*g*-PE-PyN	2	M	1.1	0.70	6.1	0.22	27	0.07	101	0.01		1.12
		E	24.8	0.48	55.6	0.47	130	0.05			0	1.17
	4	M	0.8	0.77	5.1	0.17	27	0.05	99	0.01		1.19
		E	27.2	0.43	55.1	0.52	123	0.04			0	1.05
	8	M	0.7	0.80	4.2	0.16	21	0.04	71	0.01		1.17
		E	13.1	0.35	37.7	0.57	87	0.08			0	1.23
	10	M	0.8	0.77	5.2	0.17	25	0.06	86	0.01		1.09
		E	18.1	0.36	44.5	0.58	100	0.06			0	1.10
	12	M	1.0	0.74	5.7	0.18	26	0.06	88	0.01		1.06
		E	17.3	0.26	44.1	0.64	96	0.10			0	1.17
	16	M	1.0	0.78	5.5	0.15	25	0.06	77	0.01		1.16
		E	13.4	0.35	39.0	0.58	91	0.07			0	1.13

decays, but no photophysical basis exists presently to assign the exact origin of the decay times presented in Table 2. The ratio of the sum of the negative pre-exponential factors over the sum of the positive pre-exponential factors, namely, the A_{E-}/A_{E+} ratio, was calculated. An A_{E-}/A_{E+} ratio of −1.0 indicates that excimer formation proceeds uniquely from the encounter of an excited pyrene with a ground-state pyrene, whereas an A_{E-}/A_{E+} ratio of 0.0 indicates that all excimer is produced via direct excitation of pyrene aggregates.[10,11] The rise time in the excimer decay is more pronounced the closer to −1.0 the A_{E-}/A_{E+} ratio is. In all excimer decays, little to no rise time (see A_{E-}/A_{E+} ratios in Table 2) was observed, indicating that excimer formation occurs instantaneously via direct excitation of pyrene aggregates.

When discussing A_{E-}/A_{E+} ratios, the temporal resolution of the settings used to operate the time-resolved fluorometer needs to be considered to correlate the value of an A_{E-}/A_{E+} ratio with the presence of pyrene aggregates. Pyrene aggregates such as those generated by association of a pyrene-labeled poly(acrylic acid) (Py-PAA) in water/dioxane mixtures can be shown to form excimer with A_{E-}/A_{E+} ratios close to −1.0 if the excimer decays are acquired with an ultrashort time per channel (TPC < 1 ps/ch) to probe the fast rearrangement of the pyrene moieties involved in a pyrene aggregate.[20] The TPCs of 1.02 and 2.04 ns/ch used in the present study to acquire, respectively, the pyrene excimer and monomer decays would not resolve the subnanosecond rise time observed with Py-PAA. Excimer decays of Py-PAA acquired with a 1.02 ns/ch TPC would yield an A_{E-}/A_{E+} ratio equal to zero, which based on earlier discussion would imply that the pyrene pendants are aggregated as observed experimentally. The largest A_{E-}/A_{E+} ratio in Table 2 equals −0.19, much smaller than −1.0, which is taken as an indication that little pyrene excimer is formed by diffusion in the dry films.

The kinetics of pyrene excimer formation for pyrene-labeled macromolecules are well understood in organic solvents where the Birks scheme,[21,22] compartmental analysis,[23−26] Fluorescence Blob Model,[27] or Model Free analysis[28,29] can be applied depending on the selected macromolecule and mode of pyrene attachment. Pyrene aggregation in organic solvents or aqueous

dx.doi.org/10.1021/jp208646b | J. Phys. Chem. B 2012, 116, 6203−6214

solution has been investigated, and a few mathematical treatments have been proposed to handle the kinetics of excimer formation under such conditions.[12,13,30−32] In comparison, quantitative analysis of the kinetics of pyrene excimer formation in solid polymer films labeled with pyrene is poorly developed, and studies presenting fluorescence decays of pyrene-labeled polymer matrices provide typically a qualitative interpretation of the sum of exponentials analysis of the decays.[16,33−35] This state of affair is probably a result of the absence of long-range chain motions in solid-state samples which prevents diffusive excimer formation. Diffusive excimer formation in solution enables one to couple parts of the monomer decay with the rise time of the excimer decay resulting in retrieval of similar decay times in the sum of exponentials analysis of the monomer and excimer decays. As the A_{E-}/A_{E+} ratios equal or close to zero in Table 2 made clear, the solid-state polymer films AC-*g*-PE-PyBu and AC-*g*-PE-PyN with hardly any excimer formation by diffusion yield different sets of decay times indicating that the photophysical processes undergone by the pyrene monomer and excimer are essentially uncoupled and reflect the local environment probed by pyrene in the polymer matrix. If an excited pyrene were to probe a homogeneous environment, a monoexponential decay would be expected. None of the decay analyses carried out with the films resulted in a monoexponential decay, indicating that these films are not homogeneous at the length scale of a pyrene molecule as could be expected from blends of PE and poly(methyl acrylate).

However, a measure of the relative local heterogeneity of the environment probed by an excited pyrene monomer can be obtained by monitoring the polydispersity index (PDI) of the pyrene monomer decays, namely, the ratio of the weight-average ($\langle\tau\rangle_W$) and number-average ($\langle\tau\rangle_N$) lifetime. A PDI = $\langle\tau\rangle_W/\langle\tau\rangle_N$ ratio equal to unity reflects a monoexponential decay and a homogeneous environment of the pyrene monomer. PDIs listed in Table 3 are equal to 1.4 ± 0.1 and 7.8 ± 1.7 for the AC-*g*-PE-PyBu and AC-*g*-PE-PyN films, respectively. On the basis of this observation, the AC-*g*-PE-PyN films appear to provide a much more heterogeneous environment to the pyrene labels than the AC-*g*-PE-PyBu films do.

Table 3. Number-Average ($\langle\tau\rangle_N$) Lifetimes, Weight-Average ($\langle\tau\rangle_W$) Lifetimes, and Polydispersity Index of the Decays ($\langle\tau\rangle_W/\langle\tau\rangle_N$) of the Monomer Decays

label	dose (kGy)	$\langle\tau\rangle_N$ (ns)	$\langle\tau\rangle_W$ (ns)	$\langle\tau\rangle_N/\langle\tau\rangle_W$
PyBu	2	111	151	1.4
PyBu	4	109	146	1.3
PyBu	8	67.2	104	1.6
PyBu	10	95.8	128	1.3
PyBu	12	81.3	107	1.3
PyBu	16	70.0	95.2	1.4
PyN	2	5.1	32.3	6.3
PyN	4	3.9	36.5	9.3
PyN	8	2.5	25.6	10.2
PyN	10	3.9	30.2	7.7
PyN	12	4.6	29.6	6.4
PyN	16	4.1	26.4	6.4

The $\langle\tau\rangle_N$ values are equal to 89 (±20) and 4 (±1) ns for the AC-*g*-PE-PyBu and AC-*g*-PE-PyN films, respectively. They are thus much smaller for the AC-*g*-PE-PyN films, suggesting that the matrix of the AC-*g*-PE-PyN films does not stabilize the excited pyrene monomer effectively, a possible consequence of heterogeneity. The reason for the enhanced heterogenity of the AC-*g*-PE-PyN films will become clear in the following sections.

Excimer formation is usually described using the I_E/I_M ratio, where I_E and I_M are the pyrene excimer and monomer fluorescence intensities, respectively. In numerous cases, the I_E/I_M ratio for pyrene-labeled polymers is well described by the relationship given in eq 4.[36]

$$\frac{I_E}{I_M} \propto k_{diff} \times [Py]_{loc} \tag{4}$$

In eq 4, k_{diff} and $[Py]_{loc}$ represent the bimolecular rate constant of excimer formation (typically by a diffusive process) and the pyrene concentration experienced locally by an excited pyrene, respectively. Since the samples AC-*g*-PE-PyBu yield no excimer, the I_E/I_M ratio equals 0 whereas it is infinite for the AC-*g*-PE-PyN samples that do not show monomer emission. Having established the values of the I_E/I_M ratio for both samples, eq 4 can now be applied to determine which parameter might be inducing the effect seen in Figure 6. Since both samples were in the dry state to acquire the fluorescence spectra, k_{diff} is expected to be infinitely small for both polymer matrices. The parameter that affects the process of excimer formation in the film must thus be $[Py]_{loc}$, being very large in the AC-*g*-PE-PyN films and much smaller in the AC-*g*-PE-PyBu films. Yet the pyrene-labeled poly(methyl acrylate) grafted onto the PE plates has a similar pyrene content (Table 1), which suggests that the enhancement in $[Py]_{loc}$ expected to take place in the AC-*g*-PE-PyN films has another root. That root might be the cross-linking of the poly(methyl acrylate) chains grafted with 1-pyrenemethylamine, which would bring the pyrene labels closer to each other, resulting in an enhanced $[Py]_{loc}$. To investigate the likelihood of this possibility, swelling experiments were conducted.

Swelling Behavior of the Polymers. Polymer films were soaked for a minimum of 24 h in acetone, a selective solvent for the poly(methyl acrylate) chains grafted to the PE films. A small but fluorescently non-negligible amount of free pyrene species was detected in the acetone supernatant. To eliminate these fluorescent impurities, the films were transferred to vials containing fresh solvent. This process was repeated until the steady-state emission of pyrene measured in the supernatant was low enough to be comparable to the background signal collected with a fluorescence cell filled with acetone and excited at 344 nm. Quantification of the amount of pyrene label that was released from the films indicated that it represented less than 0.3 mol % of the total pyrene content of the film. These quantities are too small to possibly affect the conclusions reached earlier with the dry films. The supernatants of the highly grafted AC-*g*-PE-PyBu (*γ*-irradiation doses of 12 and 16 kGy) polymers showed both excimer and monomer emission. Gel permeation chromatography was used to separate the components of the supernatant and confirmed the presence of monomeric pyrene as well as pyrene-labeled polymeric chains with high molecular weight (between 275 and 430 kg/mol). AC-*g*-PE-PyN supernatants exhibited only pyrene monomer emission and did not contain free chains, likely due to those chains being bound to the film via intermolecular cross-links. The photophysical behavior of the acetone-swollen films will be discussed at a later stage.

The swelling ratio of the polymer films, expressed as the mass of the acetone-swollen films over their dry mass, increased

dx.doi.org/10.1021/jp208646b | J. Phys. Chem. B 2012, 116, 6203−6214

as the grafting level increased for the AC-*g*-PE-PyBu samples as shown in Figure 7. They were conducted at two different time

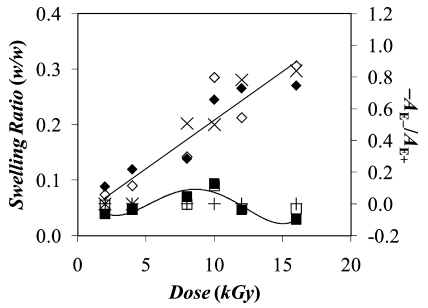

Figure 7. Swelling ratios of the AC-*g*-PE-PyBu (diamonds) and AC-*g*-PE-PyN (squares) films in acetone plotted as a function of irradiation dosage. Filled and hollow symbols represent experiments that were conducted after 1 and 7 days, respectively. Ratio A_{E-}/A_{E+} is shown on the secondary axis for the PyBu (×) and PyN (+) samples.

intervals, namely, after 1 and 7 days. The reproducibility of the results indicates that the swelling ratios shown in Figure 7 describe equilibrium conditions. The AC-*g*-PE-PyN films showed significantly less swelling than their AC-*g*-PE-PyBu counterparts with a local maximum at 10 kGy. Higher grafting levels resulted in a reduced swelling ratio. The poor swelling of the AC-*g*-PE-PyN films confirms formation of intra- and intermolecular cross-links via formation of imide bonds with the higher grafting levels allowing more cross-links to form.

Photophysical Properties of the Grafted Polymers in Acetone. Steady-state fluorescence measurements of the AC-*g*-PE-PyBu and AC-*g*-PE-PyN films were performed and are shown in Figure 8. Spectra of the AC-*g*-PE-PyBu films shown in Figure 8A yielded predominantly monomer emission, but increasing grafting levels resulted in the appearance of a clearly distinguishable pyrene excimer emission. This trend is shown in the inset of Figure 8A, where the I_E/I_M ratio is plotted as a function of irradiation dosage. It suggests that the pyrene-labeled poly(methyl acrylate) chains are solvated by acetone, which allows them to form excimer via diffusion. The fluorescence spectra of AC-*g*-PE-PyN films are shown in Figure 8B. The AC-*g*-PE-PyN swollen films exhibited mainly excimer emission with only the lowest grafting levels exhibiting any residual monomer emission.

In order to get a more detailed understanding of the process of excimer formation in the swollen films, the fluorescence decays of the pyrene monomer and excimer were acquired for all films swollen in acetone (Figure 9). The pre-exponential factors and decay times retrieved from multiexponential analysis of the fluorescence decays are listed in Table 4. As for the fluorescence decays acquired with the dry films, the fits of the decays with a sum of exponentials cannot give a full explanation of the data as no photophysical basis for interpretation of the decays has been provided, but they provide important qualitative information about the composition of the films. The fluorescence decays of the pyrene excimer of the samples AC-*g*-PE-PyBu-16kGy dry, AC-*g*-PE-PyN-16kGy dry, AC-*g*-PE-PyBu-16kGy in acetone, and AC-*g*-PE-PyN-16kGy in acetone are shown in Figure 9A, 9B, 9C, and 9D, respectively.

The acetone-swollen AC-*g*-PE-PyBu samples that did not show excimer formation in Figure 8A had excimer decays with no rise time. However, the AC-*g*-PE-PyBu that exhibited some excimer emission in Figure 8A, i.e., those samples generated with a larger irradiation dosage, all had a pronounced rise time characteristic of excimer formation by diffusion (compare Figure 9A and 9C). This observation demonstrates that as acetone swells the films it solvates the pyrene-labeled poly(methyl acrylate) chains whose recovered mobility enables excimer formation by diffusion. On the other hand, no rise time was observed in any of the AC-*g*-PE-PyN samples either in the dry or in the acetone-swollen state (compare Figures 9B and 9D).

According to its definition, the A_{E-}/A_{E+} ratio which is used to describe the magnitude of the rise time in the excimer decays reflects the mobility of the pyrenyl groups covalently attached onto a polymer.[10,11] It is thus quite remarkable that the A_{E-}/A_{E+} ratio of the swollen films plotted as a function of radiation dose was found to track closely the swelling ratio shown in Figure 7. Both parameters reflect the solvation of the pyrene-labeled poly(methyl acrylate) grafted onto the PE plates, the swelling and the A_{E-}/A_{E+} ratio providing information at the macroscopic and molecular level, respectively.

Scanning Electron Microscopy. SEM experiments were conducted to investigate whether the nature of the pyrene derivatives used in the labeling reaction would affect the morphology of the films. To this end, the films that were irradiated with higher doses of γ-rays were freeze fractured in liquid nitrogen and the aromatic rings of the pyrenyl derivatives present in their cross-section were stained preferentially with RuO_4.[37] Electrons that were backscattered by ruthenium were detected and resulted in the lighter areas shown in Figure 10. The unstained polyethylene matrix appeared as the darker domains. The bright areas observed on the edges of the film in Figure 10E are due to electron built up on the films. Figure 10A

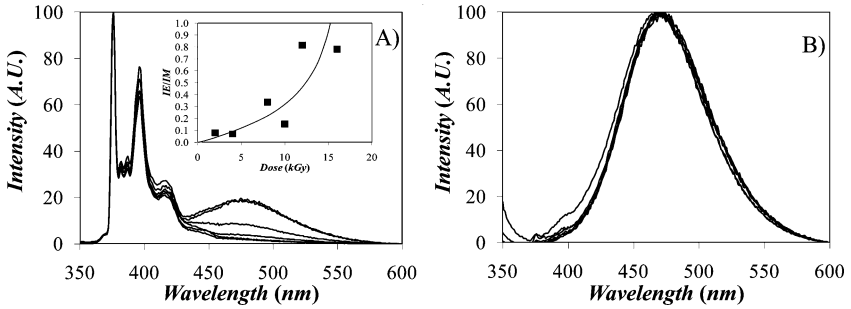

Figure 8. Fluorescence spectra of the AC-*g*-PE-PyBu (A) and AC-*g*-PE-PyN (B) films in acetone normalized at 376 and 470 nm, respectively. Inset in Figure 8A: I_E/I_M ratio as a function of dosage for the AC-*g*-PE-PyBu films in acetone. λ_{ex} = 344 nm.

dx.doi.org/10.1021/jp208646b | J. Phys. Chem. B 2012, 116, 6203–6214

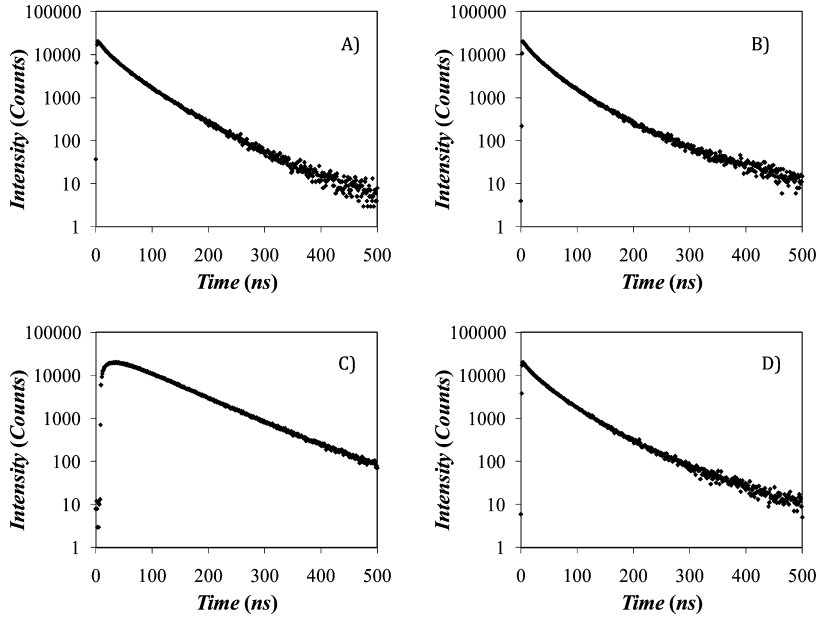

Figure 9. Excimer fluorescence decays of the dry AC-*g*-PE-PyBu-16kGy film (A), dry AC-*g*-PE-PyN-16kGy film (B), swollen AC-*g*-PE-PyBu-16kGy film (C), and swollen AC-*g*-PE-PyN-16kGy film (D). λ_{ex} = 344 nm; λ_{em} = 510 nm. Residuals and autocorrelation of residuals of these decays are provided as Supporting Information.

Table 4. Pre-Exponential and Decay Times Retrieved from Analysis of the Time-Resolved Fluorescence Decays of AC-*g*-PE-PyBu and AC-*g*-PE-PyN in Acetone with a Sum of Exponentials for the Monomer (λ_{ex} = 344, λ_{em} = 375 nm) and Excimer (λ_{ex} = 344, λ_{em} = 510 nm)

	dose (kGy)		τ_1 (ns)	A_1	τ_2 (ns)	A_2	τ_3 (ns)	A_3	τ_4 (ns)	A_4	A_{E-}/A_{E+}	χ^2
AC-*g*-PE-PyBu	2	M	7.1	0.26	61.8	0.26	156	0.48				1.14
		E	3.4	0.39	9.0	0.31	74	0.18	144	0.12	0.00	1.07
	4	M	17.6	0.19	79.6	0.33	157	0.48				0.98
		E	4.4	0.53	89.6	0.39	172	0.08			0.00	1.23
	8	M	16.5	0.29	61.0	0.40	126	0.31				1.08
		E	4.9	−0.13	21.2	−0.38	61	0.80	116	0.20	−0.51	1.25
	10	M	14.4	0.18	62.5	0.35	136	0.47				1.01
		E			32.0	−0.50	56	0.65	118	0.36	−0.50	1.15
	12	M	10.8	0.28	45.1	0.41	104	0.32				1.01
		E	5.3	−0.26	21.9	−0.52	64	0.78	106	0.22	−0.78	1.13
	16	M	12.8	0.26	48.9	0.45	96	0.29				0.99
		E	4.7	−0.21	22.1	−0.63	72	0.95	123	0.05	−0.84	1.08
AC-*g*-PE-PyN	2[a]	M										
		E	22.3	0.28	48.0	0.61	108	0.11				1.20
	4[a]	M										
		E	30.3	0.39	56.0	0.55	120	0.06				1.28
	8	M										
		E	16.0	0.32	41.0	0.59	89	0.09				1.15
	10	M										
		E	10.9	0.30	34.7	0.57	78	0.13				1.10
	12	M										
		E	20.1	0.42	49.9	0.54	119	0.04				1.29
	16	M										
		E	12.9	0.31	39.8	0.60	86	0.10				1.07

[a]Analysis of the decays was started 4 channels from the maximum of the instrument response function due to the presence of radiofrequencies at the early times of the excimer decay.

and 10C demonstrates that the edges of the films are constituted of homogeneous domains of pyrene-labeled polyacrylate and that darker PE domains are still present at the center of the films. The AC-*g*-PE-PyN-8kGy sample in Figure 10A and 10B shows more PE domains in the core of the film than AC-PE-PyN-12kGy in Figure 10C and 10D, as expected from the higher degree of AC grafting. Comparison of the cross-section of the film core obtained with the AC-*g*-PE-PyN and AC-*g*-PE-PyBu samples in Figure 10B, 10D, and 10F clearly illustrates the morphology differences between the films prepared with the two pyrene derivatives. Whereas well-separated domains of PE and pyrene-labeled poly(methyl

dx.doi.org/10.1021/jp208646b | J. Phys. Chem. B 2012, 116, 6203−6214

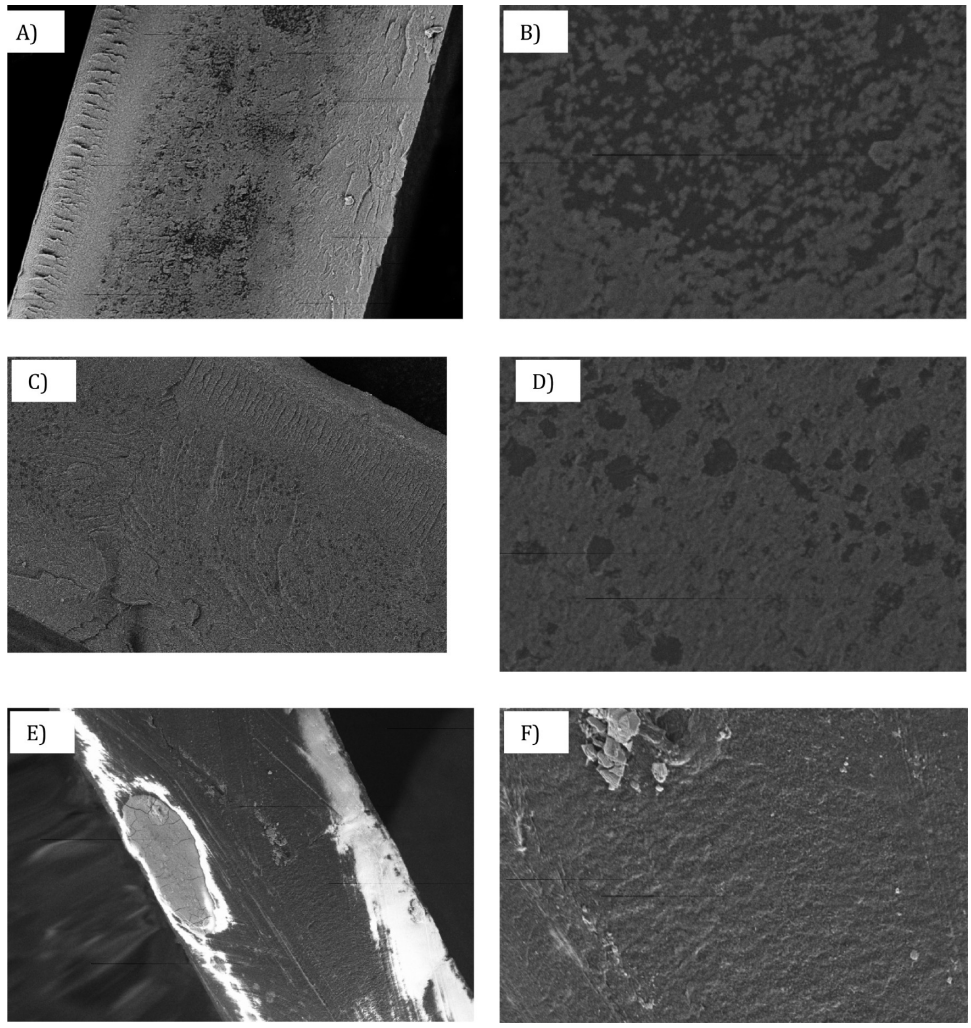

Figure 10. SEM images from fractured film samples: (A) AC-*g*-PE-PyN-8kGy, (B) AC-*g*-PE-PyN-8kGy, (C) AC-*g*-PE-PyN-12kGy, (D) AC-*g*-PE-PyN-12kGy, (E) AC-*g*-PE-PyBu-12kGy, and (F) AC-*g*-PE-PyBu-12Gy. Image widths: (A, C, and E) 185 and (B, D, and F) 26 μm.

acrylate) are easily observed in the AC-*g*-PE-PyN films, the AC-*g*-PE-PyBu films exhibit a homogeneous morphology in their core, suggesting that the 1-pyrenebutanol labels are distributed more homogeneously throughout the film. These different morphologies observed for the AC-*g*-PE-PyBu and AC-*g*-PE-PyN films are believed to be responsible for the so markedly different photophysical behavior of the films.

Physical Description of the Grafted Films. The data that were presented in this study enable a detailed description of the films. Upon irradiation of the films, initiation of the polymerization of AC can occur in the bulk or at the surface of the PE plate. Whereas the bulk of the PE plates contain many more initiation sites than their surface, accessibility to AC of the initiation sites located close to or at the surface is easier than for the sites located deep in the bulk. Indeed, Figure 10A and 10C illustrates formation of polyacrylate-rich domains at the edges of the films. However, the AC-*g*-PE-PyBu samples generated with a low irradiation dose showed very little excimer formation when the films were swollen with acetone (Figure 8A). If the chains were generated at the surface of the PE plate, excimer formation would have been observed after placing the films in acetone since acetone would solvate the chains and the resulting mobility would lead to excimer formation. That this was not observed by steady-state and time-resolved fluorescence experiments indicates that most poly(acryloyl chloride) chains are initiated in the PE plate, close to but not at the surface. Acetone, being a poor solvent for the PE matrix, cannot effectively solvate the pyrene-labeled poly(methyl acrylate) chains that are trapped in the PE matrix. Consequently, no enhancement in chain mobility is probed by our fluorescence experiments and excimer formation is not observed.

As more poly(acryloyl chloride) is grafted onto the PE plate, in particular for Grafting% greater than 100% corresponding to irradiation doses greater than 8 kGy (Figure 2), the shear mass of poly(acryloyl chloride) grafted onto the PE plate generates domains of poly(acryloyl chloride) that are now accessible to the surface of the films. After labeling with 1-pyrenebutanol, these domains can be swollen effectively by acetone as demonstrated by their increased swelling ratios (Figure 7) and mobility as described by the appearance of excimer fluorescence in the fluorescence spectra (Figure 8A) and a rise time in the excimer fluorescence decays (Figure 9C).

Labeling with 1-pyrenemethylamine of the PE plates grafted with poly(acryloyl chloride) results in cross-linking of the grafted material. The films swell little when placed in acetone (Figure 7). Cross-linking of the pyrene-labeled poly(methyl acrylate) chains enhances the local pyrene concentration which, according to eq 4, results in enhanced excimer formation, as

dx.doi.org/10.1021/jp208646b | *J. Phys. Chem. B* 2012, 116, 6203–6214

found in Figure 6B. Swelling of the films by acetone should decrease $[Py]_{loc}$ and promote excimer formation by diffusion. In turn, diffusive excimer formation should be associated with the appearance of the pyrene monomer in the fluorescence spectra and a rise time in the excimer decays. No monomer emission was observed in the fluorescence spectra of the AC-*g*-PE-PyN films in acetone (Figure 8B), and little to no rise time was observed in the fluorescence decays (Figure 9D and Table 4). These observations are a direct consequence of the cross-linking of the chains which prevents any swelling of the AC-*g*-PE-PyN films (Figure 7).

Since cross-linking of the AC-*g*-PE-PyN films occurs randomly between different and the same poly(acryloyl chloride) chains, the pyrene pendants in these films experience a heterogeneous environment over the length scale of a pyrene molecule. This local heterogeneity is reflected by the short $\langle\tau\rangle_N$ values 4 (±1) ns and the large PDIs (=7.8 (±1.7)) of the fluorescence decays of the pyrene monomer (see Table 3). By comparison, the pyrene labels in the AC-*g*-PE-PyBu films decay with longer $\langle\tau\rangle_N$'s (89 (±20) ns) and in a more monoexponential fashion with a PDI of 1.4 ± 0.1. These results suggest that the AC-*g*-PE-PyBu films exhibit a more homogeneous matrix.

The cross-linking process taking place in the AC-*g*-PE-PyN films also affects the morphology of the films. As shown by SEM, cross-linking of polyacrylate with 1-pyrenemethylamine promotes the phase separation between the polyacrylate and PE domains (Figure 10A–D), which further enhances the local pyrene concentration inside the poly(methyl acrylate) regions. In comparison, the interior of the AC-*g*-PE-PyBu films appears to be much more homogeneous (Figures 10E and 10F) with no apparent domain being formed at the magnification used for the SEM experiments. With an overall labeling level 1.9 ± 0.4 times larger than the AC-*g*-PE-PyBu samples in average, the high local pyrene concentration of the AC-*g*-PE-PyN films being further exacerbated by phase separation between the cross-linked poly(methyl acrylate) and PE domains results in an enhanced ability of the pyrene pendants to absorb light, possibly by increasing the path length of the light and thus the chance of the light being absorbed by multiple scattering at the interface between the microdomains. By concentrating the pyrene derivatives in small cross-linked polyacrylate domains, these arrays of closely packed pyrene groups are much more efficient at blocking the path of light for the AC-*g*-PE-PyN samples than they appear to be in the AC-*g*-PE-PyBu samples where 1-pyrenebutanol is more randomly distributed throughout the film (Figure 10E and 10F). They also favor excimer formation as the fluorescence spectra shown in Figures 6B and 8B confirm.

CONCLUSIONS

Control of the grafting level of the polyethylene films was obtained by varying the dose of radiation used to initiate the grafting reaction. Successful incorporation of pyrene into the grafted polymer films was confirmed by UV–vis and FTIR spectroscopy. Labeling of the films with 1-pyrenemethylamine (AC-*g*-PE-PyN series) slightly decreased the thermal stability but completely blocked the films' ability to swell in acetone. The chemically similar 1-pyrenebutanol derivative did not induce these effects as it is incapable of generating intra- and intermolecular cross-links. Fluorescence measurements were performed on dry and acetone-soaked films. Whereas substantial differences were observed between the fluorescence response of the dry and acetone-swollen AC-*g*-PE-PyBu films notably in terms of diffusive excimer formation, no noticeable difference was observed for the AC-*g*-PE-PyN. This behavior is fully consistent with the absence and presence of cross-linking, respectively. Cross-linking of the poly(acryloyl chloride) domains in the PE matrix induces formation of well-separated domains of cross-linked polyacrylate and PE (Figure 10A–D) resulting in a large local concentration of 1-pyrenemethylamine. In turn, the distribution of the pyrene labels into pyrene-rich microdomains is believed to induce multiple scattering of the excitation light at the microdomain boundaries and lengthen the light path in the polymer matrix in a process that results in enhanced absorbance of the AC-*g*-PE-PyN films with respect to the AC-*g*-PE-PyBu series (Figure 5). The pyrene-rich microdomains also favored excimer formation (Figure 6).

The photophysical properties of the pyrene-labeled films described in the present study demonstrate the dramatic effect that the reactive group of a dye derivative used to label a polymer has on them. Use of a reactive group capable of cross-linking one of two polymers constituting a polymeric film appears to concentrate the dye in the domains generated by the cross-linked polymer resulting in a substantial increase in absorbance. Of particular interest was the dual use of the pyrene probe as an indicator of, first, polymer chain flexibility from pyrene excimer formation monitored by fluorescence and, second, polymer morphology upon staining the pyrene-labeled film with RuO_4 and studying it by electron microscopy. Combination of these two techniques was instrumental in demonstrating the compartmentalization of the polymer films into PE domains and pyrene-rich domains of cross-linked polyacrylate in the AC-*g*-PE-PyN samples. To the best of our knowledge, this report represents the first example of this dual use of pyrene. Finally, the observation that clustering of a dye in a polymer matrix results in an enhanced absorbance of the polymer film is expected to find numerous practical applications.

ASSOCIATED CONTENT

Supporting Information

Excimer decays shown in Figure 9 are presented with residuals and autocorrelation of residuals. This material is available free of charge via the Internet at http://pubs.acs.org.

AUTHOR INFORMATION

Corresponding Author

*E-mail: jduhamel@uwaterloo.ca (J.D.); burillo@nucleares.unam.mx (G.B.); riverage@iim.unam.mx (E.R.).

Notes

The authors declare no competing financial interest.

ACKNOWLEDGMENTS

We are grateful to Miguel Angel Canseco (IIM-UNAM) for his assistance with FTIR and UV–vis spectroscopy. We thank also Esteban Fregoso Israel (IIM-UNAM) for his help recording TGA and DSC. We acknowledge also Francisco García and Benjamín Leal (ICN-UNAM) for their technical assistance with irradiation of the samples. This project was financially supported by CONACYT (Project 128788), PAPIIT-DGAPA (IN-105610), and the Instituto de Ciencia y Tecnología del Distrito Federal. M.F., J.Y., and J.D. are indebted to NSERC for financial support. M.F., J.Y., and J.D. thank Dale Weber (UW)

and Nina Heinig (UW) for their help with the RuO_4 staining of the films and SEM experiments, respectively.

REFERENCES

(1) Han, M. K.; Moon, S.-H.; Sohn, I. S. US 2009/0104412.
(2) Intawiwat, N.; Pettersen, M. K.; Rukke, E. O.; Meier, M. A.; Vogt, G.; Dahl, A. V.; Skaret, J.; Keller, D.; Wold, J. P. *J. Dairy Sci.* **2010**, *93*, 1372−1382.
(3) Weaver, M. A.; Strand, M. A.; Kendrick, C. L.; Rhodes, G. F.; Williams, G.; Pearson, J. C.; Upshaw, T. A. US 2004/0087688, 2004.
(4) Hilbert, S. D.; Pruett, W. P.; Wang, R. H. S.; Weaver, M. A. WO 8604904 A1, 1986.
(5) Glossmann, H.; Hering, S.; Savchenko, A.; Berger, W.; Friedrich, K.; Garcia, M. L.; Goetz, M. A.; Liesch, J. M.; Zink, D. L.; Kaczorowskix, G. J. *Proc. Natl. Acad. Sci.* **1993**, *90*, 9523−9527.
(6) Gupta, B.; Anjum, N. *Adv. Polym. Sci.* **2003**, *162*, 35−61.
(7) Desai, S. M.; Singh, R. P. *Adv. Polym. Sci.* **2004**, *169*, 231−293.
(8) Chapiro, A. *Radiation Chemistry of Polymeric Systems*; Interscience Publishers, J. Wiley Sons: New York, 1962.
(9) Ivanov, V. S. *Radiation Chemistry of Polymers*; VSP: Utrecht, 1992.
(10) Winnik, F. M. *Chem. Rev.* **1993**, *93*, 587−614.
(11) Duhamel, J. In *Molecular Interfacial Phenomena of Polymers and Biopolymers*; Chen, P., Ed.; Woodhead Publishing Co., 2005; pp 214−248.
(12) Siu, H.; Duhamel, J. *J. Phys. Chem. B* **2008**, *112*, 15301−15312.
(13) Siu, H.; Duhamel, J. *J. Phys. Chem. B* **2012**, ASAP.
(14) Lakowicz, J. R. *Principles of Fluorescence Spectroscopy*; Plenum Press: New York, 1983.
(15) Press, W. H.; Flannery, B. P.; Teukolsky, S. A.; Vetterling, W. T. *Numerical Recipes. The Art of Scientific Computing (Fortran Version)*; Cambridge University Press: Cambridge, 1992.
(16) Matsui, J.; Mitsuishi, M.; Miyashita, T. *J. Phys. Chem. B* **2002**, *106*, 2468−2473.
(17) Aguilar-Martínez, M.; Bautista-Martínez, J. A.; Rivera, E. *Des. Monomers Polym.* **2008**, *11*, 173−186.
(18) Rivera, E.; Carreón-Castro, M. P.; Huerta, G.; Becerril, C.; Rivera, L.; Salazar, R. *Polymer* **2007**, *48*, 3420−3428.
(19) Duhamel, J. *Polymers* **2012**, *4*, 211−239.
(20) Costa, T.; Seixas de Melo, S.; Castro, C. S.; Gago, S.; Pillinger, M.; Gonçalves, I. S. *J. Phys. Chem. B* **2010**, *114*, 12439−12447.
(21) Birks, J. B. *Photophysics of Aromatic Molecules*; Wiley: New York, 1970; p 301.
(22) Winnik, M. A. *Acc. Chem. Res.* **1985**, *18*, 73−79.
(23) Zachariasse, K. A.; Duveneck, G.; Busse, R. *J. Am. Chem. Soc.* **1984**, *106*, 1045−1051.
(24) Maçanita, A. L.; Zachariasse, K. A. *J. Phys. Chem. A* **2011**, *115*, 3183−3195.
(25) Beechem, J. M.; Ameloot, M.; Brand, L. *Chem. Phys. Lett.* **1985**, *120*, 466−472.
(26) Zachariasse, K. A.; Busse, R.; Duveneck, G.; Kühnle, W. *J. Photochem.* **1985**, *28*, 237−253.
(27) Duhamel, J. *Acc. Chem. Res.* **2006**, *39*, 953−960.
(28) Siu, H.; Duhamel, J. *J. Phys. Chem. B* **2005**, *109*, 1770−1780.
(29) Yip, J.; Duhamel, J.; Bahun, G.; Adronov, A. *J. Phys. Chem. B* **2010**, *114*, 10254−10265.
(30) Seixas de Melo, J.; Costa, T.; Miguel, M. d. G.; Lindman, B.; Schillén, K. *J. Phys. Chem. B* **2003**, *107*, 12605−12621.
(31) Farinha, J. P. S; Martinho, J. M. G.; Xu, H.; Winnik, M. A.; Quirk, R. P. *J. Polym. Sci. B: Polym. Phys.* **1994**, *32*, 1635−1642.
(32) Lee, S.; Duhamel, J. *Macromolecules* **1998**, *31*, 9193−9200.
(33) Yanagimachi, M.; Toriumi, M.; Masuhara, H. *Chem. Mater.* **1991**, *3*, 413−418.
(34) Brown, G. O.; Guardala, N. A.; Price, J. L.; Weiss, R. G. *J. Phys. Chem. B* **2002**, *106*, 3375−3382.
(35) Brown, G. O.; Atvars, T. D. Z.; Guardala, N. A.; Price, J. L.; Weiss, R. G. *J. Polym. Sci. B: Polym. Phys.* **2004**, *42*, 2957−2970.
(36) Cuniberti, C.; Perico, A. *Prog. Polym. Sci.* **1984**, *10*, 271−316.
(37) Chen, J. T.; Thomas, E. L.; Ober, C. K.; Mao, G.-P. *Science* **1996**, *273*, 343−346.